

Hardware-Aware YOLO Compression for Low-Power Edge AI on STM32U5 for Weeds Detection in Digital Agriculture

Charalampos S. Kouzinopoulos and Yuri Manna

Abstract—Weeds significantly reduce crop yields worldwide and pose major challenges to sustainable agriculture. Traditional weed management methods, primarily relying on chemical herbicides, risk environmental contamination and lead to the emergence of herbicide-resistant species. Precision weeding, leveraging computer vision and machine learning methods, offers a promising eco-friendly alternative but is often limited by reliance on high-power computational platforms. This work presents an optimized, low-power edge AI system for weeds detection based on the YOLOv8n object detector deployed on the STM32U575ZI microcontroller. Several compression techniques are applied to the detection model, including structured pruning, integer quantization and input image resolution scaling in order to meet strict hardware constraints. The model is trained and evaluated on the CropAndWeed dataset with 74 plant species, achieving a balanced trade-off between detection accuracy and efficiency. Our system supports real-time, in-situ weeds detection with a minimal energy consumption of 51.8mJ per inference, enabling scalable deployment in power-constrained agricultural environments.

Index Terms—Edge Artificial Intelligence (Edge AI), Computer Vision, Deep Neural Networks (DNNs), Digital Agriculture, Tiny Machine Learning (TinyML), Internet of Things (IoT).

I. INTRODUCTION

WEEDS are widespread and persistent plants, known for their rapid reproduction and effective seed dispersal strategies. They are among the primary contributors to crop yield loss globally, posing a significant challenge for farmers and agricultural stakeholders [1]. Effective weeds management remains a critical issue, as weeds impact broader concerns related to food security, ecosystem health, and environmental sustainability [2]. Conventional weeds control strategies have traditionally relied heavily on chemical herbicides. While these methods can be effective in the short term, with a 52-96% efficacy over manual weeding [3], their widespread and indiscriminate use risks contaminating ecosystems and accelerates the emergence of herbicide-resistant weed species. As of 2024, more than 523 unique cases of weed resistance have been reported in 269 weed species [3]. Addressing this issue aligns directly with the European Green Deal's objectives of promoting sustainable food systems, reducing chemical

pesticide use, and safeguarding biodiversity, highlighting the need for innovative, eco-friendly weed control strategies [4].

Effective weed control can increase the productivity per unit area to meet the growing demand for crop production [5]. One promising solution that can be cost-effective and environmentally sustainable is to automate the weeding process through precision weeding. This technique involves the targeted identification and removal of weeds using advanced technologies such as computer vision, machine learning (ML), robotics and remote sensing. Unlike conventional blanket spraying methods, precision weeding systems can accurately distinguish between crops and weeds, enabling site-specific interventions that minimize chemical usage and reduce damage to surrounding crops and soil.

A typical weed detection system follows four key steps: image acquisition, data segmentation, feature extraction, and weed detection [6]. A novel and effective approach for the detection of weeds in image data leverages ML techniques, particularly through the use of computer vision and deep learning (DL) models. There is significant research interest in this area, with several studies demonstrating high accuracy in weed identification using convolutional neural networks (CNNs), vision transformers (ViTs) and other architectures [7][8][9]. A thorough review on the use of different DL methods for weed detection is given in [10]. However, most existing work is based on high-end computational platforms for inference, such as GPUs or cloud-based systems. These setups are not directly transferable to real-world agricultural fields, where energy efficiency, latency, cost and connectivity constraints pose significant challenges. Many rural areas lack the connectivity required to support sensor node installations, and while power may be sporadically available, it is often scarce across the broader farm landscape. This highlights the need for the design and deployment of efficient weed detection models on low-power, edge-based platforms, enabling real-time, in-situ decision-making.

The aim of this study is to develop a low-power Internet of Things (IoT) system, capable of detecting the presence of weeds in open-air fields and greenhouses, via the use of an optimized computer vision inference pipeline. The proposed pipeline is based on the YOLOv8n one-shot detector, and is executed at the edge targeting the low-power STM32U575ZI microcontroller unit (MCU) by ST Microelectronics. The key contributions of this article are as follows: 1) the development of an optimized computer vision edge AI model to enable efficient on-device execution, via the use of different model

The authors are with the Department of Advanced Computing Sciences, Maastricht University, 6229 GS, Maastricht, Netherlands. e-mail: charis.kouzinopoulos@maastrichtuniversity.nl, y.manna@student.maastrichtuniversity.nl (Corresponding author: C.S. Kouzinopoulos).

Manuscript received April 19, 2005; revised August 26, 2015.



Fig. 1. YOLOv8n detection output

compression techniques, including structured pruning, integer quantization and input data size reduction; 2) the evaluation of the model’s efficiency vs size of weights and activations on a large-scale dataset; and 3) the evaluation of the system’s energy consumption during edge inference. Figure 1 shows an example of a successful detection output.

The rest of the paper is organized as follows. Section II reviews related work on YOLO-based edge AI methods for low-power object detection as well as on different YOLO architectures for weed detection. Section III details the background and proposed methodology, including training process, pruning and quantization compression techniques as well as the hardware setup and deployment process on the STM32U575ZI MCU. Section IV evaluates the results in terms of detection accuracy, inference time, and energy consumption. Section V draws conclusions and outlines directions for future research.

II. LITERATURE REVIEW

A. Edge AI YOLO networks

The feasibility of object detection on resource-constrained, low-power MCUs is an active topic in the literature, driven by the need to bring intelligent capabilities closer to the data source and provide localized decision making. This paradigm, known as artificial intelligence (AI) at the edge or *edge AI*, involves performing inference of deep neural networks (DNNs) and other AI models directly on edge devices, without the need to offload computation to cloud servers or more powerful, energy-intensive hardware. There is a significant body of work on low-power edge AI based on CNN models and single-shot detectors. Specifically, focus is given on the compression of different YOLO (You Only Look Once) versions, a popular single-stage detector that uses CNNs for object detection and classification, for resource-constrained MCUs.

TinyissimoYOLO, a lightweight object detection network was presented in [11]. The network architecture, consisting of 422k parameters, was compressed using quantization and quantization-aware training techniques enabling deployment on different MCUs. On the ST Microelectronics STM32H7A3 and STM32L4R9 MCUs it achieved latencies of 359ms and 996ms and an energy consumption per inference of 41.8mJ and 102mJ respectively. When deployed on the AmbiQ

Apollo4b, the network had a latency of 540ms and 6.08mJ energy per inference. Finally, it was deployed on an Analog Devices MAX78000 MCU with a CNN accelerator, achieving a latency of 5.5ms with an energy consumption of 0.19mJ per inference.

A modified version of TinyissimoYOLO was introduced in [12] and was evaluated on the Greenwaves GAP9 MCU for object detection, achieving a latency of up to 16.2ms and energy consumption of up to 31 μ J per inference. Squeezed Edge YOLO, a compressed object detection model with 931k parameters for human and shape detection was proposed in [13]. The model was evaluated on a Greenwaves GAP8 MCU, achieving approximately 70.3mJ energy (541mW power) consumption and 130ms latency per inference.

μ YOLO, a custom YOLO architecture for MCUs, was introduced in [14]. The model was deployed on an OpenMV Cam H7 R2 MCU, based on an Cortex-M7 core, with memory requirements of 800 KB of flash and 350 KB of RAM. To reduce model size and computational cost, the network was pruned across all convolutional and fully connected layers during training using an $L1$ -norm heuristic, and was further compressed using 8-bit quantization. Energy consumption on the board and latency are not reported; moreover the size of parameters is not given, although it can be estimated based on the flash requirements and quantization bits to approximately 800k.

MCUBench, a large-scale benchmark of 100+ YOLO-based object detection models was presented in [15]. The models were evaluated on the Pascal VOC dataset [16] covering 20 different object classes. Performance metrics, such as average precision, latency, RAM, and flash usage were reported across various MCU families, including STM32H7, STM32F4, STM32F7, STM32L4 and STM32H5-U5.

B. YOLO-based weeds detection

Several YOLO architectures have also been implemented in the literature for the detection of weeds, although not specifically targeting low-power embedded systems. In [17], YOLO-Weed Nano was presented, a lightweight detection network based on YOLOv8n for weed recognition in cotton fields. The network had a mean Average Precision (mAP) at an intersection over union (IoU) threshold of 50 (mAP50) of 0.931, 1.09M parameters and 2.4MB weight size, achieving 4.7 GFLOPS and 227.3 frames per second (fps). An NVIDIA RTX 3090 GPU was used for the network evaluation. A lightweight YOLO-based model was introduced in [18] for weed detection, achieving an mAP50 of 0.952, a mAP at IoU thresholds from 0.50 to 0.95 (mAP50-95) of 0.889 with approximately 2.78M parameters and 9.3 GFLOPS. The model was evaluated on an NVIDIA RTX 3080 Ti GPU. YOLO-WDNet, a lightweight model based in YOLOv5 for weed detection in cotton fields was presented in [19]. The model, evaluated on an NVIDIA Jetson AGX Xavier GPU, had an mAP50 of 0.978, with 0.9M parameters and 3.1 GFLOPS.

To the best of our knowledge, this is the first study in the literature to explore compression techniques of YOLO models for weed detection specifically on low-power MCUs, such

as STM32U575ZI, enabling localized, low-power decision-making for the identification of weeds in digital agriculture.

III. METHODOLOGY

A. YOLO (*You Only Look Once*)

Traditional CNN object detectors typically follow a two-stage pipeline: first, the input image is scanned to generate region proposals; each region is then classified separately. In contrast, YOLO is a single-stage detector that processes the entire image in a single pass through convolutional layers, framing object detection as a regression problem. This approach improves significantly computational efficiency, making YOLO suitable for real-time execution in resource-constrained environments, while still achieving state-of-the-art accuracy.

For this work, three recent versions of YOLO have been initially evaluated: YOLOv8n, YOLOv10n and YOLOv11n. As detailed in section III-C1 below, YOLOv8n experienced significantly less performance degradation after pruning compared to the YOLO versions evaluated and for this reason was selected as the baseline model for this study. The architecture comprises approximately 3.2×10^6 parameters distributed across 129 layers for a total size of 9.95 MB.

YOLOv8 follows an anchor-free detection approach with different stages, where each stage typically consists of multiple convolutional blocks, producing features at a higher level of abstraction and processing data from different resolutions [20]. The model architecture is structured around three main components: the backbone for feature extraction at multiple scales, the neck for feature aggregation and the head for prediction. YOLOv8 uses a similar backbone to YOLOv5, starting with the *stem*, where two convolutional blocks convert the input into initial features and reduce its resolution. A series of Cross-stage partial bottleneck with two convolutions (C2f) blocks follow, incorporating two parallel gradient flow branches to enhance the integration of features with contextual information. They split the input feature map along the channel dimension with one part passing unchanged through an *identity connection* while the other passing through a series of lightweight bottleneck modules. A Spatial pyramid pooling - fast (SPPF) block is used to provide a multi-scale representation of the input feature maps. By pooling at different scales, SPPF allows the model to capture features at various levels of abstraction. The neck assembles feature pyramids, aggregating features from different backbone stages using up-sampling and concatenation, allowing multi-scale context capture. The head generates the final detection and classification outputs and operates on the fused feature maps to regress bounding box coordinates, confidence scores, and class labels.

B. Training

The model was trained on CropAndWeed [21], a large-scale image dataset for the fine-grained identification of crop and weed species. The dataset is composed of annotated samples from cultivation areas in Austria, as part of an *application* set, and additionally includes an *experimental* set with different

TABLE I
TRAINING AND FINE-TUNING HYPERPARAMETERS

Hyperparameter	Training	Fine-tuning
Batch size	Auto (-1)	150
Epochs	300	30
Image size	224 × 224	
Initial learning rate (lr_0)	0.001	
Final learning rate (lrf)	0.1	
Patience	50	–
Momentum	0.937	–
Optimizer	SGD	Adam
Weight decay	0.0005	–
Automatic Mixed Precision	–	True
Test-time augmentation	True	

species, specifically grown in controlled outdoor environments to enrich the dataset with underrepresented classes. It contains a collection of 74 plant species: 16 crop species, including maize, sugar, beets, beans, peas, sunflowers, soy, potatoes and pumpkins, and 58 weed species, such as grass, amaranth and goosefoot. The images cover varying conditions in terms of lighting conditions as well as soil and type.

For the model training of this work, data were used from both the *application* and *experimental* sets. More than 20.765 crops instances and 57.523 weed instances were represented. The dataset was split into training and validation sets using an 80-20 ratio. Training of the baseline model was carried out using the Ultralytics library on a NVIDIA GeForce RTX 3090 GPU using CUDA 12.2. The model was trained for 300 epochs with an input resolution of 224 × 224 pixels. All training and fine-tuning hyper-parameters used are listed in Table I.

C. Model Compression

A major challenge in deploying DNNs on low-power MCUs is meeting the strict constraints on memory, processing power and energy consumption. For the target hardware platform in this work, the model including weights must be compressed to under 2 MB to fit within the internal flash memory, while the model activations including input and output must fit within 768 KB of RAM. At the same time, it is essential to minimize the model’s energy consumption without significantly impacting detection accuracy. To address these constraints, we applied a combination of structured pruning and integer quantization. Moreover, the input data dimensions were scaled to 224 × 224 pixels to reduce computational load and memory usage.

1) *Pruning*: According to the Lottery Ticket Hypothesis [22], a randomly initialized network contains sub-networks that, when trained in isolation, can match the performance of the original network. Pruning exploits this concept by eliminating parameters, such as weights and activations, to reduce model size while maintaining target accuracy. It is important to note that filters in different network layers have varying importance to the model’s performance [23], while aggressive pruning, especially on critical layers such as attention modules, may significantly reduce performance. Pruning is often followed by fine-tuning to improve network accuracy.

There are two main approaches to network pruning, *unstructured* or *weight pruning* and *structured* or *channel pruning*. In

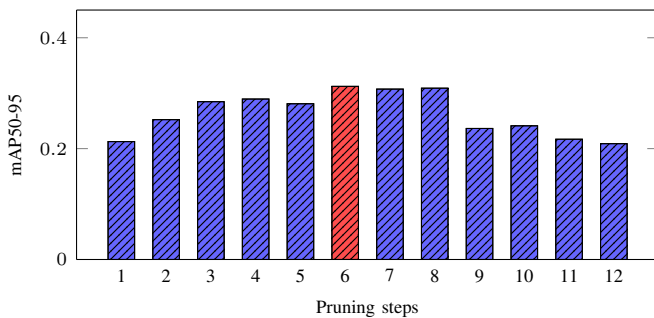


Fig. 2. Effect of k on model accuracy for a 70% pruning ratio

unstructured pruning individual weights are removed in a fine-grained way, resulting in a sparse model. However, this often requires specialized hardware to benefit from the sparsity. *Structured* pruning on the other hand involves the removal of entire neurons or filters, preserving the original connectivity and maintaining the dense structure of the network, so that further optimizations can be easily implemented without any specialized hardware units [24]. In this work, pruning is applied to entire convolutional filters and channels, since that way a considerable pruning ratio can usually be achieved with little performance degradation [25].

The structured pruning implementation of this work is based on Torch-Pruning [26], an open-source pruning library that automatically traces and maintains model dependency graph. To determine which filters to prune, *local pruning* or *global pruning* can be used. With *local pruning*, parameter importance is evaluated within the current layer while with *global pruning*, a global ranking of all parameters is performed. The importance evaluation is commonly performed using $L2$ norm. The $L2$ norm of a weight vector $w = (w_1, \dots, w_n)$ measures its magnitude and is defined as:

$$\|w\|_2 = \sqrt{\sum_{i=1}^n w_i^2} \quad (1)$$

To reach target sparsity, an iterative pruning schedule is selected to gradually prune the model, while allowing the network training steps to recover from any pruning-induced loss in accuracy. This approach is generally considered to achieve better accuracy than aggressive one-shot pruning, especially at higher pruning ratios [27], as it allows access to narrow, well-generalizing minima, which are typically ignored when using one-shot approaches [28]. Given a target pruning ratio r_{target} and a total number of steps k , the pruning fraction per step is calculated using a progressive geometric decay schedule as:

$$\text{pruning per step} = 1 - (1 - r_{target})^{\frac{1}{k}} \quad (2)$$

Following this schedule, the network is pruned rapidly in the initial phase when the redundant connections are abundant while the number of weights to be pruned are gradually reduced following each step as there are fewer remaining in the network [29].

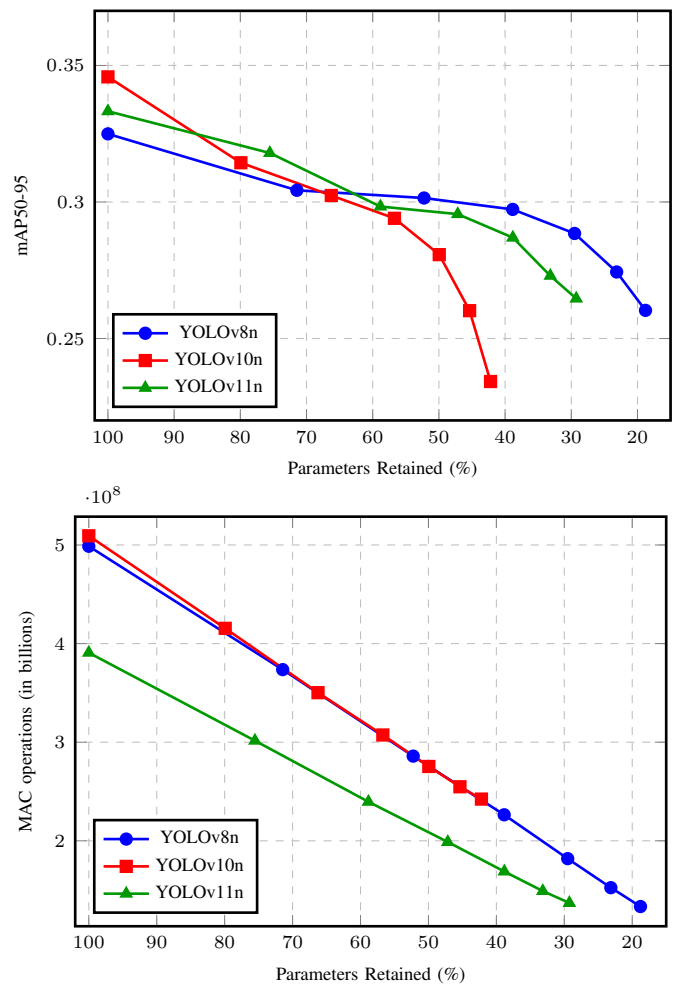


Fig. 3. Effect of pruning on a) accuracy and b) inference complexity, for YOLOv8n, YOLOv10n and YOLOv11n

As depicted on Figure 2, the network accuracy was evaluated for a pruning ratio of 70%, for $k \in \{1, \dots, 12\}$. It can be seen that $k = 6$ offers the best tradeoff between accuracy and training speed and was thus used for the rest of this work's experiments. The pruning process begun with the pre-processing and validation of the model to establish a baseline for accuracy. Concatenation and detection layers were excluded due to their sensitivity to parameter reduction. At each iteration, the least important filters were pruned based on their $L2$ norm ranking, followed by fine-tuning the network for 30 epochs to recover any accuracy loss. This cycle was repeated until the desired pruning ratio was reached or a predefined accuracy drop threshold of 20% was met, in terms of mAP. The output of this process is a *float32* model in *onnx* format.

As can be seen in Figure 3 (a), YOLOv8n demonstrated significantly higher robustness to pruning compared to YOLOv10n and YOLOv11n, with a notably lower performance degradation. Consequently YOLOv8n was selected as the baseline architecture for subsequent optimization experiments. Performance evaluation indicates that up to 60% of the network's parameters can be effectively pruned with an mAP loss of 0.1 compared to the unpruned model. A pruning

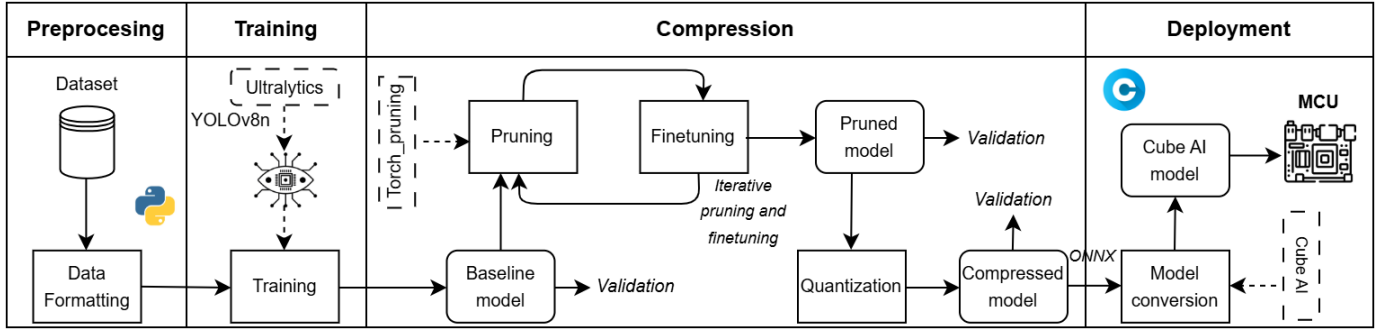


Fig. 4. Diagram of the preprocessing, training, compression and deployment pipeline used.

ratio of 70% pruning leads to a 0.15 loss, which is still within acceptable limits for this scenario. However, more aggressive pruning results in a notable accuracy degradation, indicating a threshold beyond which the model no longer maintains sufficient representational capacity. Figure 3 (b) depicts a near-linear correlation between the number of pruned parameters and the reduction in computational cost measured in multiply-accumulate (MAC) operations.

Based on the evaluation steps above, a pruning ratio of 70% was selected, leading to a total of 960k parameters for the network.

2) *Quantization*: Quantization is one of the most widely adopted techniques for improving the efficiency of edge AI models and ML accelerators [30]. It reduces the numerical precision of model parameters and activations, typically converting 32-bit floating-point numbers into 8-bit integers or lower. This results in a memory overhead reduction by a factor of $4\times$ for tensor storage, while the computational cost for matrix multiplications is reduced quadratically by a factor of 16 [31]. Additionally, integer operations consume considerably less energy than their floating-point counterparts [32].

The core idea behind quantization is to map real-valued numbers to a finite set of discrete levels using a linear transformation, also known as an affine mapping. This process is referred to as *linear quantization*, which can be further categorized into *asymmetric* and *symmetric uniform quantization* schemes. In asymmetric uniform quantization, the quantization process is defined as [33]:

$$\begin{aligned} \bar{x} &= \text{clamp}\left(\left\lfloor \frac{x}{s} \right\rfloor - \lfloor z \rfloor, 0, 2^b - 1\right) \\ s &= \frac{\theta_{max} - \theta_{min}}{2^b - 1} \\ z &= \frac{\theta_{min}}{s} \end{aligned} \quad (3)$$

where x is the original real value input, \bar{x} is the quantized integer output, $[\theta_{min}, \theta_{max}]$ is the quantization range and b is the target bit width. The clamp function ensures that the output is within the target range and is defined as:

$$\text{clamp}(x; a, c) = \begin{cases} a, & x < a \\ x, & a \leq x \leq c \\ c, & x > c \end{cases} \quad (4)$$

Scale s , typically stored in a float 32-bit format, determines the quantization granularity, while zero-point z (an integer) shifts the quantized range to best approximate 0 in the original domain. To recover an approximate real value \hat{x} from the quantized integer, a de-quantization step is performed:

$$\hat{x} = s(\bar{x} + \lfloor z \rfloor) \quad (5)$$

There are different approaches and design decisions that revolve around the selection of optimal quantization parameters s and z for weights and activations. The first decision concerns the choice of granularity [34]: *Per-tensor* quantization shares s and z across the entire tensor. In *per-channel* quantization for weights or *per-token* quantization for activations, s and z are shared within each row of tensor. Finally, *per-group* quantization further reduces the degree of parameter sharing by using different s and z for every g columns within each row, where g is the group size.

The next step is the definition of the range estimation method, i.e. the strategy to define θ_{min} and θ_{max} . A simple range estimation method is the *min-max* strategy, which sets θ_{min} and θ_{max} to the minimum and maximum values of the input data to cover the whole dynamic range of the tensor. While this method ensures full range coverage, it is highly sensitive to outliers. An alternative method is to minimize the *mean squared error (MSE)* between the original and quantized tensors, which yields tighter bounds, mitigating the impact of large outliers. The optimization problem of minimizing MSE is frequently solved using grid search. In certain cases, where all tensor values are not equally important, it can be effective to minimize the *cross-entropy loss* instead, which focuses on preserving classification accuracy by emphasizing the most relevant logits.

There are two primary quantization workflows. In *post training quantization (PTQ)*, weights are quantized ahead of time and the per-activation dynamic range is computed at runtime. In *static PTQ*, both weight and activation tensors are quantized ahead of time. Since the activation tensors are not known at that stage, a small calibration dataset is required, to estimate activation ranges. *Quantization-aware training (QAT)* simulates quantization effects during training using fake quantization operators (quantizer blocks), allowing the network to learn robustness to quantization noise. QAT typically leads to higher accuracy and supports more

aggressive quantization schemes. A common practice is to apply per-channel or symmetric quantizers for the weights and asymmetric quantizers for the activations [31].

Symmetric quantization is a simplified version of the general asymmetric case, where the zero-point is fixed to 0, eliminating thus the offset-related computational overhead during the accumulation operation [31]. While less flexible, this approach is computationally cheaper and is frequently used for weight quantization.

For this work, the *onnxruntime.quantization* library was used to apply *static* PTQ. A calibration dataset of 300 samples was used to estimate activation ranges. Initially, the *onnx* model obtained after pruning was pre-processed to prepare it for quantization. The quantization was performed using the Quantize-DeQuantize (QDQ) format, which inserts *QuantizeLinear* and *DeQuantizeLinear* blocks around tensors to simulate low-precision inference. The *min-max* range estimation strategy was used to determine the *s* and *z* parameters. To preserve model performance, only the convolutional, multiplication and addition operators were quantized. An asymmetric uniform quantization scheme was used for activations, while a symmetric scheme was applied to weights. Additionally, per-channel quantization was enabled for weights to improve accuracy and reduce quantization-induced degradation.

D. Deployment

For the conversion of the compressed *onnx* model into optimized c code, the proprietary STM32Cube.AI toolchain was used, an extension library of STM32CubeMX by ST Microelectronics. Table II lists the memory and processing requirements of the final compressed network, after applying the model compression techniques detailed in section III-C above, and compares them to the original YOLOv8n model and the MCU specifications.

TABLE II
COMPRESSION RESULTS

Metric	Baseline YOLOv8n	Compressed YOLOv8n	HW constraints
Model size (Flash)	9.95 MB	850.97 KB	2 MB
RAM usage	2.5 MB	677.30 KB	768 KB
Parameters	3200M	960k	-
GMACs	0.50	0.143	-

The compressed model was deployed on the NUCLEO-U575ZI-Q system-on-chip (SoC), integrating the STM32U575ZI MCU. The MCU features a 32-bit ARM Cortex-M33 core, with 2 MB of flash memory and 786 KB of SRAM. The core has a very low energy profile, with a $8.95\mu\text{A}$ current consumption at Stop 2 mode and $19.5\mu\text{A}$ per MHz run mode at 3.3V according to the device datasheet. For this deployment, the MCU was clocked at 160 MHz via the Multi-Speed Internal oscillator (MSI). The internal low-power Real-Time Clock (RTC) of the MCU was used for time keeping purposes clocked through the Low-Speed Internal oscillator (LSI) at 32 kHz. The integrated SMPS regulator was used for voltage and current control. All unused GPIOs were set to reset state to minimize leakage

currents. The Hardware Abstraction Layer (HAL) library of the STM32CubeMX by ST Microelectronics was utilized to program the SoC. To ensure accurate current consumption measurement, the on-board LD5 LED was de-soldered as it was not controllable through software.

Upon power up, the board initializes all required peripherals and begins inference. After each inference cycle, the system enters Stop 2 mode via the *HAL_PWREx_EnterSTOP2Mode()* HAL instruction combined with the Wait For Interrupt (WFI) flag. The system exits Stop 2 and resumes operation through a periodic interrupt, triggered every 30 seconds by the RTC, upon which it re-initializes and repeats the inference process.

Figure 4 depicts a complete diagram of the proposed preprocessing, training, compression and deployment pipeline used in this work.

IV. DISCUSSION

This section presents an evaluation of the proposed compressed network deployed on the STM32U575ZI MCU. The CropAndWeed dataset was used for benchmarking, with an 80 - 20 training and validation split. Performance metrics include mAP50-95, the number of model parameters (M), latency per inference (ms), frame rate (fps) and energy consumption per inference.

TABLE III
COMPARISON OF THE PROPOSED NETWORK WITH EXISTING YOLO IMPLEMENTATIONS FOR WEEDS DETECTION

Work	Detector	Device	mAP50	mAP50-95	Params (M)	Input size
[17]	YOLO-Weed Nano	RTX 3090	0.931	-	1.09	640 × 640
[18]	EcoWeedNet	RTX 3080 Ti	0.952	0.889	2.78	640 × 640
[19]	YOLO-WDNet	Jetson AGX Xavier	0.978	-	0.9	640 × 640
This work	YOLOv8n	STM32U575ZI	0.517	0.403	0.96	224 x 224

A. Model Performance Analysis

Table III presents the accuracy metrics of the proposed detection model when deployed for inference at the edge, as well as a comparison with recent state-of-the-art YOLO-based approaches for the detection of weeds. While prior works such as YOLO-Weed Nano [17], EcoWeedNet [18], and YOLO-WDNet [19] achieve high detection accuracy, with mAP50 scores exceeding 93%, these models are designed for deployment on high-end platforms that lack stringent constraints on memory, power consumption, and compute resources. Indicatively, YOLO-Weed Nano has memory requirements for 2.4MB for the network weights, while EcoWeedNet consists of triple the number of parameters as that of the proposed model.

Furthermore, the proposed model uses a significantly lower input resolution of 224×224 pixels to accommodate the limited memory specifications of the STM32U575ZI MCU. This contrasts with the 640×640 resolution used in most state-of-the-art works. Lower input resolution severely reduces spatial detail and limits the model's ability to detect small

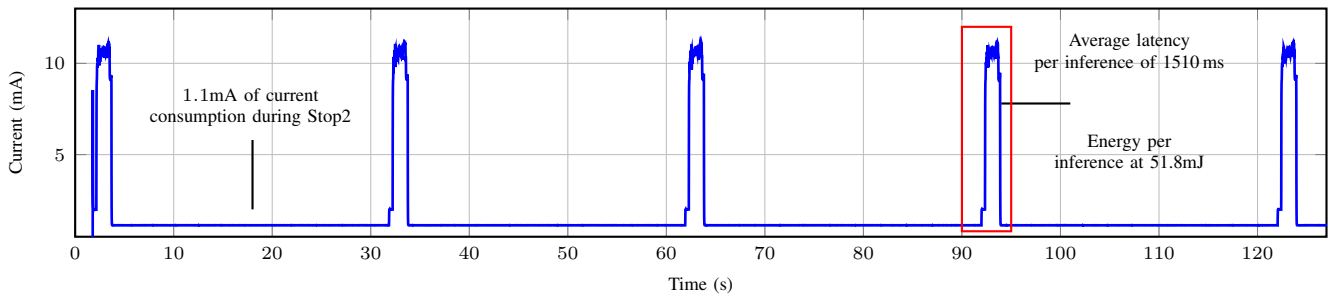


Fig. 5. Aggregated current draw of the system for 2 mins.

or partially occluded objects, leading to a significant drop in detection accuracy.

Despite these limitations, the compressed model achieved a respectable mAP50 of 0.517 and an mAP50-95 of 0.403, which are sufficient for the detection of weeds in both open-air fields and greenhouses, where low-power operation outweighs the need for state-of-the-art accuracy.

B. Energy Requirements

The current consumption of the SoC was measured using Nordic Semiconductor Power Profiler Kit II (PPK2). PPK2 is a standalone unit supporting measurements from 200nA up to 1A, with a resolution between 100nA to 1mA depending on the range, for a supply voltage of 0.8V - 5V VCC. The MCU of this work was powered through the PPK2 using a 3.3V supply voltage through a dedicated 3V3 pin.

until re-activated through an RTC interrupt. Entering deep sleep between inference cycles significantly reduces total system energy consumption, enabling longer operation. Using a 3.7V Li-Ion battery with 7000mAh (25.9Wh) the system can operate approximately for 189 days of continuous operation, under ideal assumptions, without any human intervention.

A comparison of the proposed model of this work with compressed YOLO models from the literature for low-power embedded systems is given in Table IV. As can be seen from the Table, the proposed model of this work contains a significantly larger number of parameters, contributing to improved representational power. Despite the increased complexity, our system consumes 51.8mJ per inference, remaining competitive in terms of energy. However, this comes at the cost of higher latency at 1510ms, resulting in a lower throughput of 0.66fps.

TABLE IV
COMPARISON OF THE PROPOSED YOLOV8N NETWORK WITH EXISTING LOW-POWER YOLO IMPLEMENTATIONS

Work	Detector	Device	Params (k)	Energy	Latency (ms)	Frame rate (fps)
[11]	Tinyissimo YOLO	STM32H7A3,	422	41.8mJ,	359,	2.79,
		STM32L4R9,		102mJ,	996,	1,
		Apollo4b,		6.08mJ,	540,	1.85,
		MAX78000		0.19mJ	5.5	181.82
[12]	Tinyissimo YOLO-based	GAP9	-	31μJ	16.2	61.3
[13]	Squeezed Edge YOLO	GAP8	931	70.3mJ	130	7.69
This work	YOLOv8n	STM32U575ZI	960	51.8mJ	1510	0.66

Figure 5 presents the system’s current draw over a 2-minute operation window. During active inference, the system operates continuously, achieving an average latency of 1510ms per inference, which corresponds to a frame rate of approximately 0.66 fps. The average current measured over a complete inference cycle was 10.4mA. The energy required for a single inference, given a supply voltage of 3.3V, is then computed as:

$$\begin{aligned}
 E &= V \times I \times t \\
 &= 3.3 \times 10.4 \times 10^{-3} \times 1.510 \\
 &= 51.8mJ
 \end{aligned}
 \tag{6}$$

In low-power Stop 2 mode, the MCU operates with an average current draw of approximately 1.1mA for 30 seconds,

V. CONCLUSIONS

This work presents an optimized low-power computer vision pipeline for the detection of weeds in digital agriculture, leveraging structured pruning, post-training quantization, and input resolution scaling to compress the YOLOv8n detector for efficient deployment on the STM32U575ZI MCU.

The compressed model achieves a substantial reduction in model size, from 9.95 MB to 850.97 KB, and a memory footprint that fits within the 2 MB flash and 768 KB SRAM constraints of the target hardware. Despite these aggressive optimizations, the system retains a respectable detection performance with an mAP50 of 0.517 and mAP50-95 of 0.403 on the CropAndWeed dataset, which is acceptable for many real-world agricultural settings.

In terms of energy and latency, the proposed system achieves inference at 51.8mJ in active mode and a frame rate of 0.66 fps, making it suitable for periodic monitoring tasks in power-constrained edge deployments in both open-air fields and greenhouses.

Future work will explore the integration of hardware accelerators, the use of additional network compression techniques including low rank approximation and transfer learning, as well as the use of Neural Architecture Search to further enhance model energy consumption while maintaining detection accuracy.

The authors commit to provide full access to the project source code after publication of the manuscript.

REFERENCES

- [1] M. Junaid and A. Gokce, "Global agricultural losses and their causes," *Bulletin of Biological and Allied Sciences Research*, vol. 2024, no. 1, pp. 66–66, 2024.
- [2] M. Vasileiou, L. S. Kyrgiakos, C. Kleisiari, G. Kleftodimos, G. Vlontzos, H. Belhouchette, and P. M. Pardalos, "Transforming weed management in sustainable agriculture with artificial intelligence: A systematic literature review towards weed identification and deep learning," *Crop Protection*, vol. 176, p. 106522, 2024.
- [3] T. K. Das, B. Behera, C. P. Nath, S. Ghosh, S. Sen, R. Raj, S. Ghosh, A. R. Sharma, N. T. Yaduraju, A. Nalia *et al.*, "Herbicides use in crop production: An analysis of cost-benefit, non-target toxicities and environmental risks," *Crop protection*, vol. 181, p. 106691, 2024.
- [4] European Commission, "The european green deal," 2025, https://commission.europa.eu/strategy-and-policy/priorities-2019-2024/european-green-deal_en [Accessed: 30-05-2025].
- [5] E.-C. Oerke and H.-W. Dehne, "Safeguarding production—losses in major crops and the role of crop protection," *Crop protection*, vol. 23, no. 4, pp. 275–285, 2004.
- [6] S. Shanmugam, E. Assunção, R. Mesquita, A. Veiros, and P. D. Gaspar, "Automated weed detection systems: A review," *KnE Engineering*, pp. 271–284, 2020.
- [7] M. D. Bah, A. Hafiane, and R. Canals, "Deep learning with unsupervised data labeling for weed detection in line crops in uav images," *Remote sensing*, vol. 10, no. 11, p. 1690, 2018.
- [8] S. Xie, C. Hu, M. Bagavathiannan, and D. Song, "Toward robotic weed control: detection of nutsedge weed in bermudagrass turf using inaccurate and insufficient training data," *IEEE Robotics and Automation Letters*, vol. 6, no. 4, pp. 7365–7372, 2021.
- [9] J. Yu, S. M. Sharpe, A. W. Schumann, and N. S. Boyd, "Deep learning for image-based weed detection in turfgrass," *European journal of agronomy*, vol. 104, pp. 78–84, 2019.
- [10] H.-R. Qu and W.-H. Su, "Deep learning-based weed–crop recognition for smart agricultural equipment: A review," *Agronomy*, vol. 14, no. 2, p. 363, 2024.
- [11] J. Moosmann, M. Giordano, C. Vogt, and M. Magno, "Tinyssimoyolo: A quantized, low-memory footprint, tinymml object detection network for low power microcontrollers," in *2023 IEEE 5th International Conference on Artificial Intelligence Circuits and Systems (AICAS)*. IEEE, 2023, pp. 1–5.
- [12] L. Boyle, J. Moosmann, N. Baumann, S. Heo, and M. Magno, "Dsrt-mcu: Detecting small objects in real-time on microcontroller units," *IEEE Sensors Journal*, 2024.
- [13] E. Humes, M. Navardi, and T. Mohsenin, "Squeezed edge yolo: Onboard object detection on edge devices," *arXiv preprint arXiv:2312.11716*, 2023.
- [14] M. Deutel, C. Mutschler, and J. Teich, "microyolo: Towards single-shot object detection on microcontrollers," *arXiv preprint arXiv:2408.15865*, 2024.
- [15] S. Sah, D. C. Ganji, M. Grimaldi, R. Kumar, A. Hoffman, H. Rohmetra, and E. Saboori, "Mcbenchmark: A benchmark of tiny object detectors on mcus," 2024. [Online]. Available: <https://arxiv.org/abs/2409.18866>
- [16] M. Everingham, S. A. Eslami, L. Van Gool, C. K. Williams, J. Winn, and A. Zisserman, "The pascal visual object classes challenge: A retrospective," *International journal of computer vision*, vol. 111, pp. 98–136, 2015.
- [17] J. Wang, Z. Qi, Y. Wang, and Y. Liu, "A lightweight weed detection model for cotton fields based on an improved yolov8n," *Scientific Reports*, vol. 15, no. 1, p. 457, 2025.
- [18] O. H. Khater, A. J. Siddiqui, M. S. Hossain, and A. El-Maleh, "Ecweednet: A lightweight and automated weed detection method for sustainable next-generation agricultural consumer electronics," *arXiv preprint arXiv:2502.00205*, 2025.
- [19] X. Fan, T. Sun, X. Chai, and J. Zhou, "Yolo-wdnet: A lightweight and accurate model for weeds detection in cotton field," *Computers and Electronics in Agriculture*, vol. 225, p. 109317, 2024.
- [20] P. Hidayatullah, N. Syakrani, M. R. Sholahuddin, T. Gelar, and R. Tubagus, "Yolov8 to yolov11: A comprehensive architecture in-depth comparative review," 2025. [Online]. Available: <https://arxiv.org/abs/2501.13400>
- [21] D. Steininger, A. Trondl, G. Croonen, J. Simon, and V. Widhalm, "The cropandweed dataset: A multi-modal learning approach for efficient crop and weed manipulation," in *Proceedings of the IEEE/CVF Winter Conference on Applications of Computer Vision (WACV)*, January 2023, pp. 3729–3738.
- [22] J. Frankle and M. Carbin, "The lottery ticket hypothesis: Finding sparse, trainable neural networks," *arXiv preprint arXiv:1803.03635*, 2018.
- [23] B. Wang and V. Kindratenko, "R1-pruner: Structured pruning using reinforcement learning for cnn compression and acceleration," *arXiv preprint arXiv:2411.06463*, 2024.
- [24] M. Kokhazadeh, G. Keramidas, V. Kelefouras, and I. Stamoulis, "Denseflex: A low rank factorization methodology for adaptable dense layers in dnns," in *Proceedings of the 21st ACM International Conference on Computing Frontiers*, 2024, pp. 21–31.
- [25] Z. Wang, C. Li, and X. Wang, "Convolutional neural network pruning with structural redundancy reduction," in *Proceedings of the IEEE/CVF conference on computer vision and pattern recognition*, 2021, pp. 14 913–14 922.
- [26] G. Fang, X. Ma, M. Song, M. B. Mi, and X. Wang, "Depgraph: Towards any structural pruning," in *Proceedings of the IEEE/CVF Conference on Computer Vision and Pattern Recognition*, 2023, pp. 16 091–16 101.
- [27] M. Janusz, T. Wojnar, Y. Li, L. Benini, and K. Adamczewski, "One shot vs. iterative: Rethinking pruning strategies for model compression," 2025. [Online]. Available: <https://arxiv.org/abs/2508.13836>
- [28] E. Tartaglione, A. Bragagnolo, and M. Grangotto, *Pruning Artificial Neural Networks: A Way to Find Well-Generalizing, High-Entropy Sharp Minima*. Springer International Publishing, 2020, p. 67–78. [Online]. Available: http://dx.doi.org/10.1007/978-3-030-61616-8_6
- [29] M. Zhu and S. Gupta, "To prune, or not to prune: exploring the efficacy of pruning for model compression," 2017. [Online]. Available: <https://arxiv.org/abs/1710.01878>
- [30] M. Verhelst, L. Benini, and N. Verma, "How to keep pushing ml accelerator performance? know your rooflines!" *IEEE Journal of Solid-State Circuits*, 2025.
- [31] M. Nagel, M. Fournarakis, R. A. Amjad, Y. Bondarenko, M. Van Baalen, and T. Blankevoort, "A white paper on neural network quantization," *arXiv preprint arXiv:2106.08295*, 2021.
- [32] M. Horowitz, "1.1 computing's energy problem (and what we can do about it)," in *2014 IEEE international solid-state circuits conference digest of technical papers (ISSCC)*. IEEE, 2014, pp. 10–14.
- [33] B. Jacob, S. Kligys, B. Chen, M. Zhu, M. Tang, A. Howard, H. Adam, and D. Kalenichenko, "Quantization and training of neural networks for efficient integer-arithmetic-only inference," in *Proceedings of the IEEE conference on computer vision and pattern recognition*, 2018, pp. 2704–2713.
- [34] Y. Lin, H. Tang, S. Yang, Z. Zhang, G. Xiao, C. Gan, and S. Han, "Qserve: W4a8kv4 quantization and system co-design for efficient llm serving," 2025. [Online]. Available: <https://arxiv.org/abs/2405.04532>



Charalampos S. Kouzinopoulos is an Assistant Professor of the Internet of Things and Coordinator of the Computer Systems Research Area in the Department of Advanced Computing Sciences of the Faculty of Science and Engineering at Maastricht University. He was a Senior Research Fellow at the ALICE experiment of CERN and a Senior Researcher at CERN/ITI.

His research interests lie in hardware design and integration, in software-hardware co-design and low-power edge AI, in computer architecture, parallel and distributed computing and in GPGPU computing.



Yuri Manna holds a BSc in Data Science and Artificial Intelligence from Maastricht University. His research focuses on AI systems, embedded and edge computing, and agricultural applications of artificial intelligence.